nature portfolio

https://doi.org/10.1038/s41596-021-00631-0

Supplementary information

Fabrication and use of silicon hollow-needle arrays to achieve tissue nanotransfection in mouse tissue in vivo

In the format provided by the authors and unedited

Supplementary Manual

Fabrication of Silicon Hollow Needle Arrays for Tissue Nanotransfection Applications

Yi Xuan[1,2]‡, Subhadip Ghatak[1‡], Andrew Clark[1], Zhigang Li[2], Savita Khanna[1], Dongmin Pak[3], Mangilal Agarwal[4], Sashwati Roy[1,5], Peter Duda[6], and Chandan K. Sen[1,2]**

1) Lithography

The main parameters for lithography are photoresist thickness, bake temperature and time, expose time, and develop time. Detailed technical parameters can be found on the websites provided by the chemical companies (Microchemical and Kayaku Advanced Materials). The photoresist thickness can be measured by Reflectometry, or by Surface Profilometer with patterned photoresist on the wafer. Other techniques are imaging the cross-sectional view by SEM or optical microscope after cleaving the wafer. The measurement of the photoresist thickness is important to calculate the etch rate during the process development.

2) Bosch process for etching microneedles on the frontside

First, pattern several Si wafers with SPR 220 photoresist as shown in Steps 1A xvii-xxi. Start with a standard Bosch recipe to etch a patterned wafer and frequently stop the etching process to monitor the wafer using optical microscopy, filmetric and surface profilometer[1,2].

Etching Selectivity: The surface profilometer provides the depth information. When the etching depth has reached to about 100 µm, measure the depths at several different points, and then remove the photoresist per Step 1A xxv. The depths are measured again at the same positions to calculate the Si etching rate, photoresist etching rate, and etching uniformity. If the SPR photoresist etched too fast, reduce the etching ICP power to below 1200 W, and/or reduce the bias below 30 W. The photoresist is required to remain on the wafer until an etch depth of 200 µm. The SPR photoresist has a good etching selectivity with a Bosch etch process[3]. If there is a limitation to improve the selectivity, spin-coating thicker photoresist is recommended. The SPR 220-7.0 can be coated on a wafer with over 10 µm thickness in a single coat with good uniformity.

Etching Profile: After etching about 200 µm, cleave the wafer and take cross-sectional images by SEM to identify the etching profile and quality. If it is negative as shown in Supplementary Figure 1d, reduce the etching gas (SF_6), and/or reduce the etching ICP power. In a similar way, reduce the passivation gas (C_4F_8), and/or reduce the passivation ICP power for the positive profile as shown in Supplementary Figure 1e. The tolerance of the etching angle is $\Theta = 90° \pm 2°$.

Aspect Ratio Dependent Etch (ARDE) is a serious limitation in Bosch process where the etch depth decreases with reducing feature sizes due to reactant-transport into and reaction product transport out of the narrow gap are hindered[4]. The mass transport decreases sharply with increasing aspect ratio and can even fall to zero etch rate at the critical aspect ratio. Consequently, the etch depth of D1 and D2 are very different as shown in Supplementary Figure 1c. The aspect ratio varies from 10 to 20 if the W1 changes from 10 µm to 5 µm. The ARDE can be improved by increasing SF_6 flow rate, etch bias, and reducing pressure[5,6]. Meanwhile, another easy way to achieve 100 µm of D2 etching is to reduce the aspect ratio, for example, increasing the W1 to 10 µm or 15 µm.

Grass formation: During Bosch etch process, residual polymer left on the bottom surface act as an etching mask to form grass which is a silicon column structure as shown in Supplementary Figure 1f. This grass can be eliminated by reducing C_4F_8 flow rate and/or passivation ICP power, increasing the etch bias, and 3-step process[1]. Refer to the Bosch etch process trends summarized in Supplementary Table 1.

3) Bosch process for etching reservoirs on the backside:

This process creates the hollow channels on the backside which serve as a reservoir to store DNA or genes. The optimization procedure is similar to that of the frontside. First, prepare several Si wafers that were patterned with 50 µm thick SU8 photoresist (Steps 1A ix-xiii). Then, etch the wafer to about 430 µm using the Bosch process recipe developed for the frontside. The etch rate decreases over time in high aspect ratio structures due to ARDE.[1] To reach the target value of 430 µm, increasing the etching gas (SF_6) and bias are recommended to improve the ARDE. If the etching selectivity drops due to high bias, increase the SU8 thickness to 60 µm or further as needed. Reducing the aspect ratio is a simple way to achieve the target etching depth with less effort in tuning the recipe. The hollow diameter can be changed from 20 µm to 30 µm in the GDS file which drops the aspect ratio from 21.5 to 14.3. The hollow channels on the backside serve as a reservoir to store DNA or genes, and hence the diameter and volume are not critical factors for TNT applications. The most critical process is etching through the wafer to connect the two hollow channels on the frontside and the backside so that DNA or gene can freely flow from the backside reservoir to the target tissue. The etching depth can be simply measured by an optical microscope after cleaving the wafer as shown in Supplementary Figure 2b.

Supplementary Table 1. Process trends in Bosch process[1,2]

Parameters		Etch rate	Selectivity	Profile	Sidewall Roughness	Grass	ARDE*
Step 1 Passivation	↑ C4F8 flow or time	↓↔	↑	↔	↓	↑	X
	↑ ICP power	↓↔	↑↔	Positive	↓	↑	X
Step 2 De-passivation (for 3-step Bosch)	↑ Ar	↔	↓	↔	↔	↓	O
	↑ Bias	↔	↓	↔	↔	↓	O
Step 3 Etch	↑ SF6 flow or time	↑↑	↑	negative	↑	↓	O
	↑ Etch ICP power	↑	↑	negative	↑	↓	O
	↑ Bias	↑↔	↓	↔	↔	↓	O
↑ Chamber pressure		↑↑	↑	negative	↑	↓↔	X

increase (↑), decrease (↓), no effect or negligible effect (↔), ARDE: aspect-ratio dependent etching, improve (O)

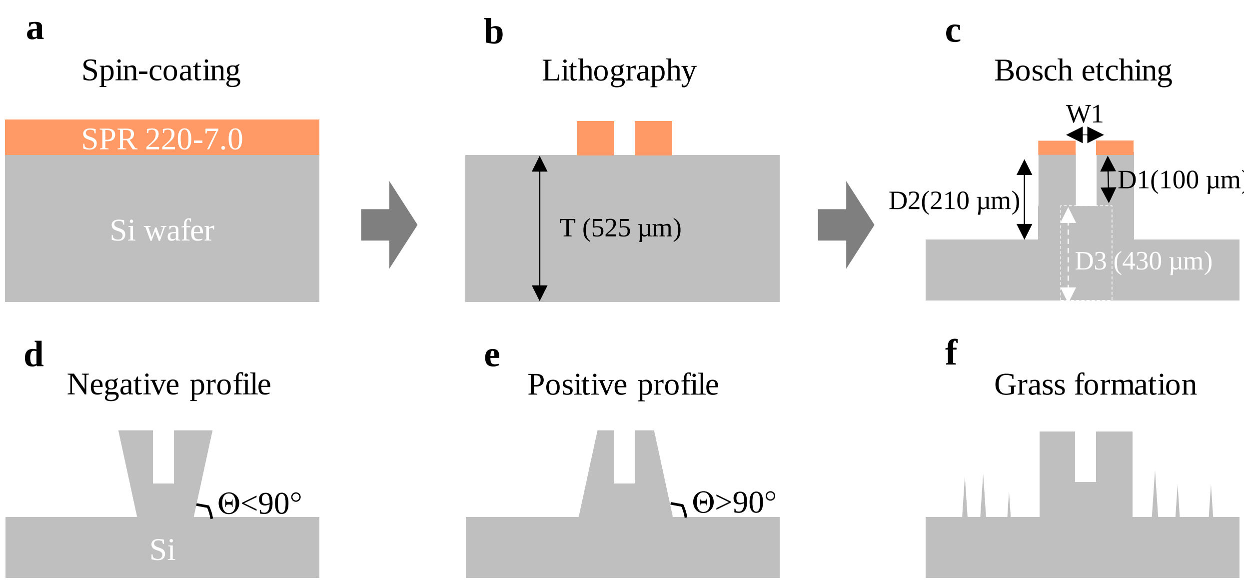

Supplementary Figure 1. Optimization of Bosch process for etching hollow microneedle arrays on the frontside. (a) spin coating SPR photoresist, (b) patterning, (c) Bosch process, (d) negative etching profile, (d) positive etching profile, (f) Grass formation.

4) SiO_2 PECVD for tuning the nozzle size:

The PECVD coating is another critical process which determines the final nozzle size for the hollow microneedle. The negatively charged DNA or genes are accelerated by the electric field and ejected from this nozzle to the tissue. The ejected speed increases with decreasing the nozzle size in a certain range. There should be a correlation between nozzle size, needle length, electric field, ejected speed, delivery distance, and delivery amount. First, prepare several Si wafers with ~ 200 µm etch depth with hollow and trench arrays using Steps 1A ix-xvi. The sizes are measured

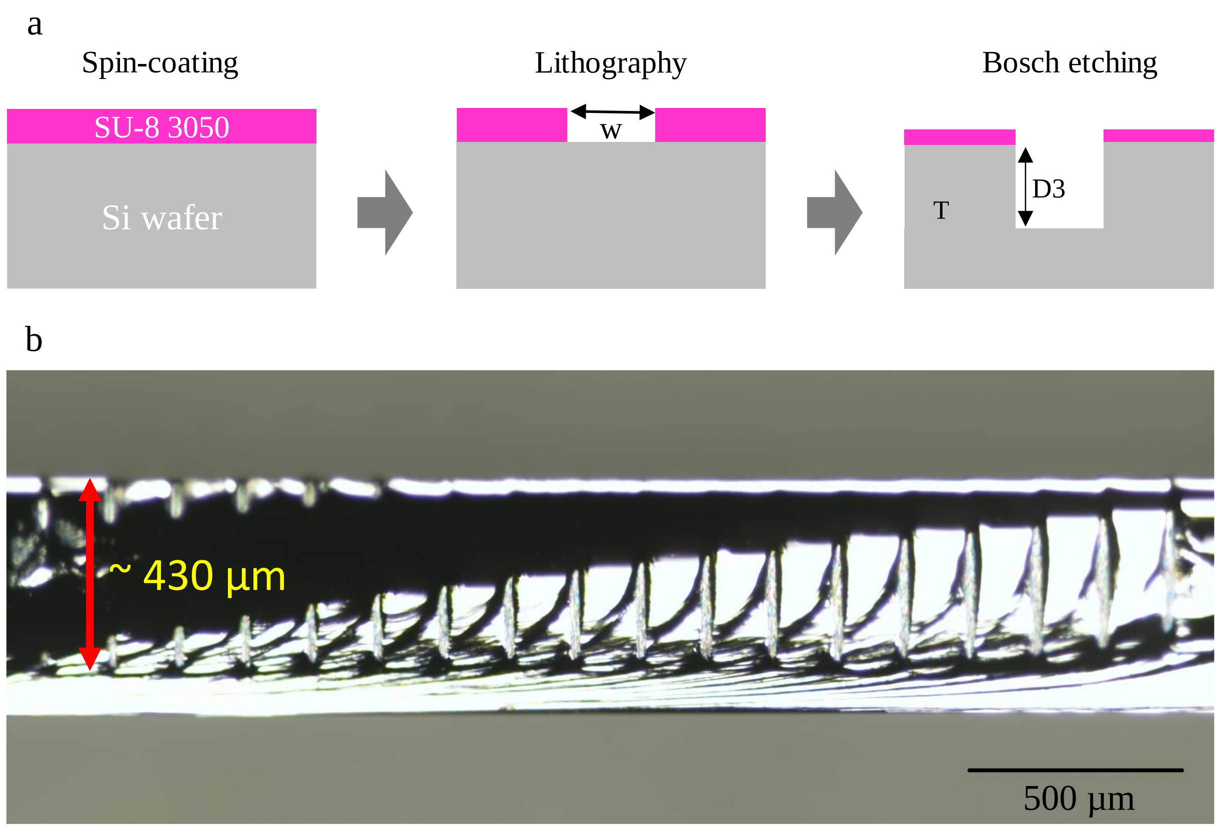

Supplementary Figure 2. Optimization of Bosch process for backside hollow etching. (a) prepare several Si wafers with 50 µm thick SU-8 pattering for Bosch process optimization. (b) A cross-sectional optical image for a quick measurement of the etching depth.

using top-view SEM imaging. Then, use a PECVD tool to deposit a layer of SiO_2. Remeasure the sizes using SEM to calculate the shrink rate as shown in Supplementary Figure 3a. The oxide thickness is measured by Filmetric tool to calculate the deposition rate. The wafer is cleaved, and the step-coverage is investigated by cross-sectional SEM imaging. As shown in Supplementary Figure 3b of a cross-sectional image, the PECVD oxide does not cover the trenches conformally. The oxide is much thinner on the sidewall compared to the top surface due to a poor step-coverage for the high-aspect ratio trenches. This non-uniform deposition helps tune the hollow sizes for TNT applications. If the oxide is uniformly deposited into the inner structure, the DNA flow rate would be reduced, and the transfection efficiency would be limited. The PECVD process trends are summarized in Supplementary Table 2.

Supplementary Table 2. PECVD process trends for SiO_2

Parameters	Deposition rate	Uniformity
↑ SiH_4 flow	↑↑	↓↓
↑ Plasma power	↑	↓↔
↑ Pressure	↓	↑
↑ Temperature	↑	

Increase (↑), decrease (↓), No effect or negligible effect (↔)

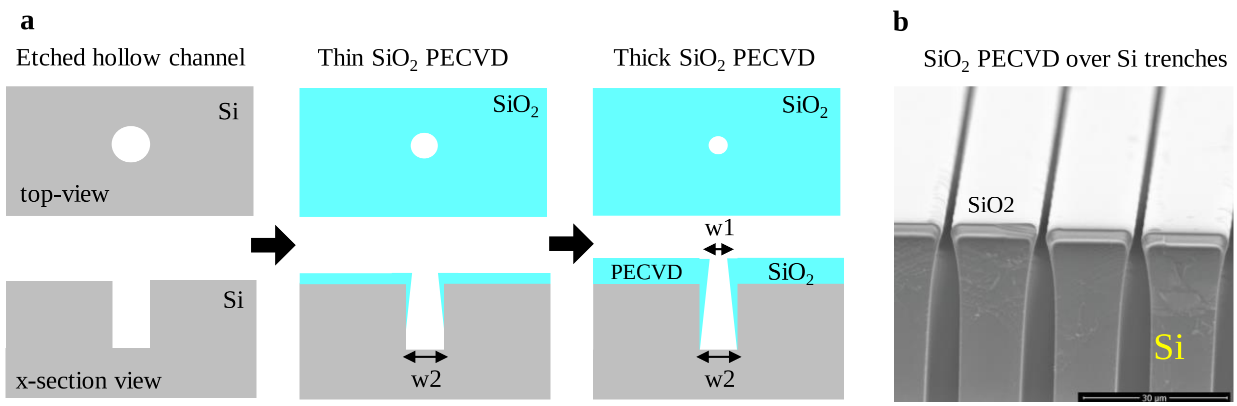

Supplementary Figure 3. Optimization of SiO_2 coating with PECVD. (a) Shrinking the hollow microchannels with SiO_2 PECVD, (b) A cross-sectional SEM image showing poor step-coverage of SiO_2 PECVD over microtrenches.

5) Mechanical Test for TNT Chips:

Mechanical property is crucial to TNT chip being used in the tissue transfection experiment. The TNT chip is mainly made from Si, a kind of fundamental material in the semiconductor industry. Supplementary Figure 4 shows the TNT chip evaluated through the loaded weights. Solid aluminum block with a weight of 1.35 Kg (13.24 N) was loaded on the top surface of the TNT chip one by one. A total weight of 5.40 Kg (52.96 N) was loaded on the chip finally, yielding a pressure of about 0.65 MPa. As seen in the SEM images (Supplementary Figure 4c - d) taken before and after the loading, respectively, there is no obvious change on the TNT chip, indicating the strong strength of the microneedles. This result guarantees the TNT treatment in practical clinic applications in the future.

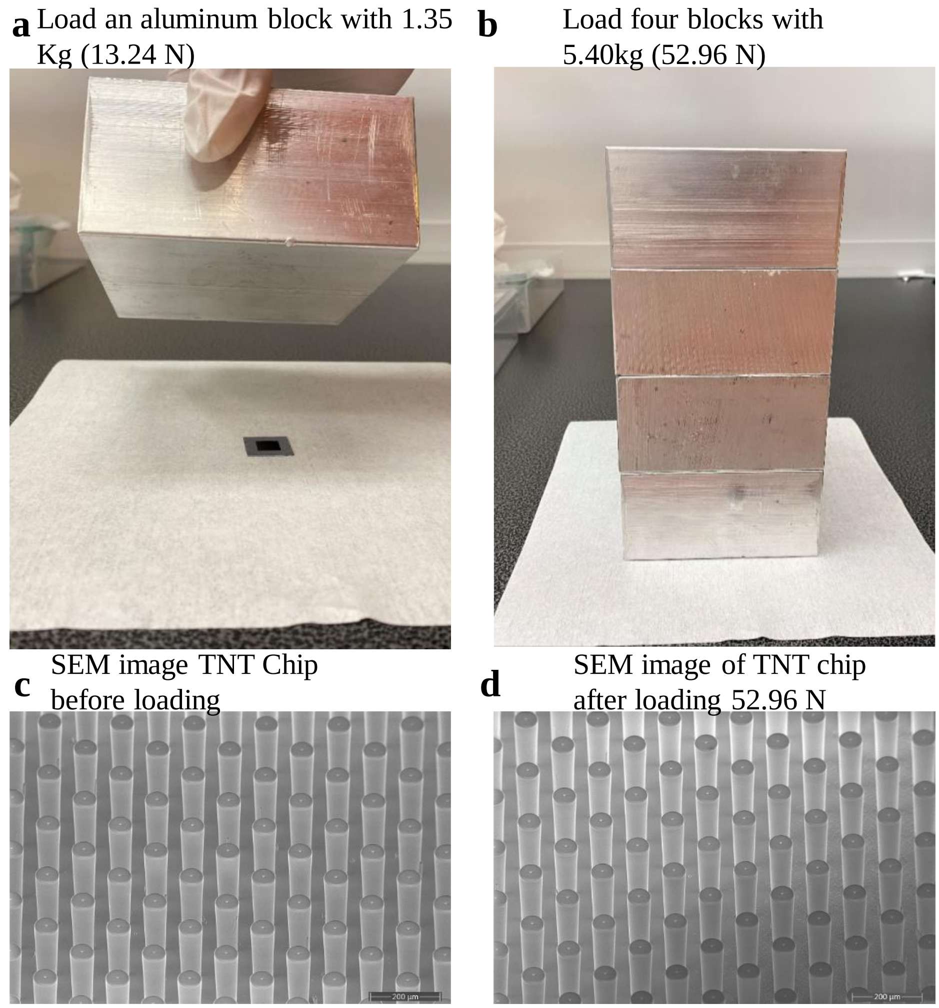

Supplementary Figure 4. Mechanical test for TNT chips

6) Force Measurement of TNT Chip During Operation

A force sensitive resistor (Pololu) was wired to a microcontroller (Arduino UNO, Elegoo) to measure the force exerted on the TNT chip during operation. One end was connected to the 5V power pin on the microcontroller the other to a 10KΩ pull-down resistor connected to the ground pin. The point between the fixed pulldown resistor and the variable force sensitive resistor was connected to the analog input of the microcontroller. As pressure is applied to the force sensitive resistor the resistance decreases, lowering the total resistance of the FSR and the pulldown resistor from 100 KΩ to 10 KΩ. The current flowing through both resistors increases which in turn causes the voltage across the fixed 10KΩ resistor to increase. Voltage was converted to conductance

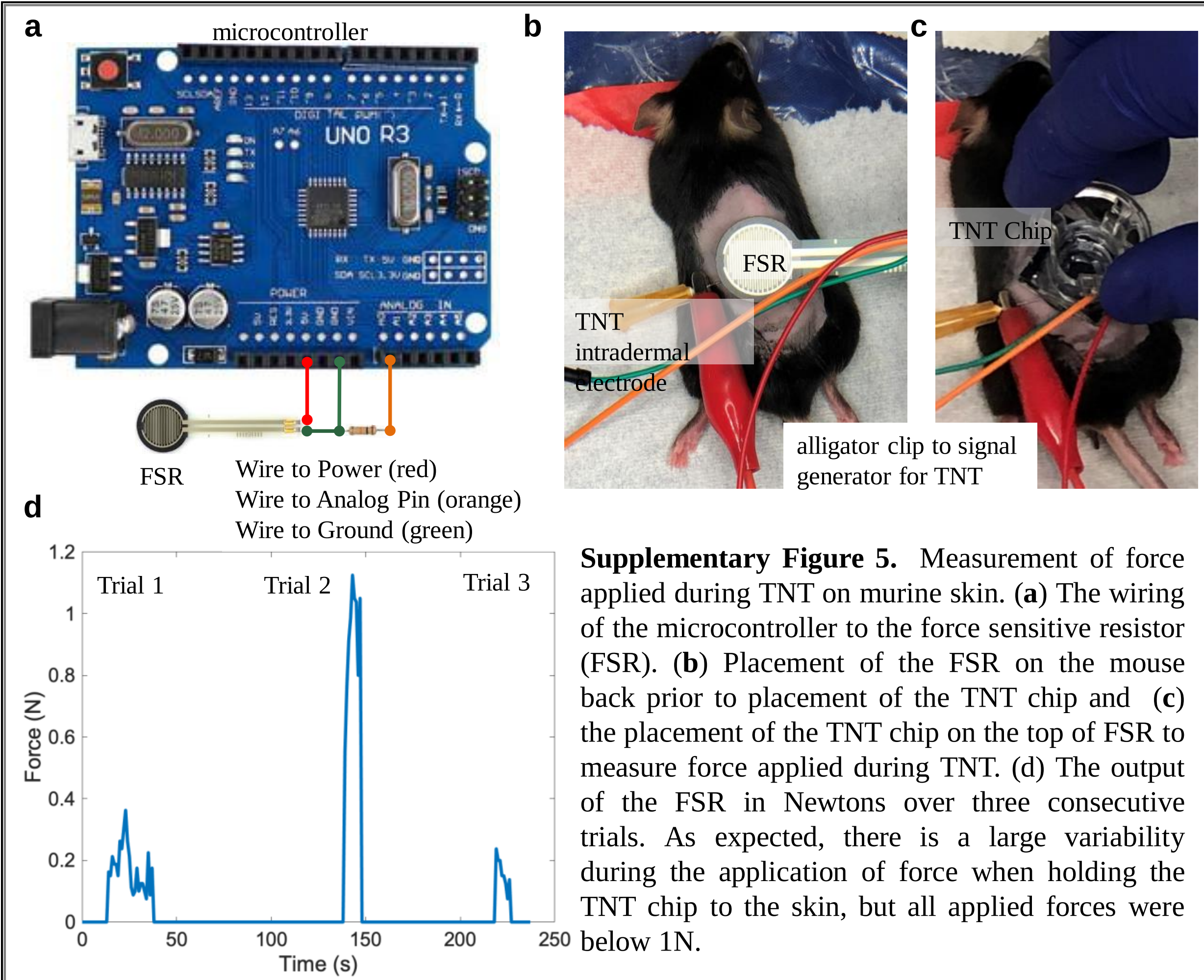

Supplementary Figure 5. Measurement of force applied during TNT on murine skin. (**a**) The wiring of the microcontroller to the force sensitive resistor (FSR). (**b**) Placement of the FSR on the mouse back prior to placement of the TNT chip and (**c**) the placement of the TNT chip on the top of FSR to measure force applied during TNT. (d) The output of the FSR in Newtons over three consecutive trials. As expected, there is a large variability during the application of force when holding the TNT chip to the skin, but all applied forces were below 1N.

which was subsequently converted to force in Newtons using the provided force sensitive resistor guide graphs (Supplementary Figure 5).

The Arduino IDE (Adafruit) was used to compile code for signal generation and data retrieval. The code was modified from the "Using a Force Sensitive Resistor" tutorial sketch on the manufacturer's website. The code can be found below. It should be noted that the force in Newtons reported by the code is rounded to the nearest integer which results in readings of zero Newtons when the force is below 0.5 N. This was rectified in postprocessing, where the conductance values were converted to force values and stored in a csv file for potting in MATLAB.

MATLAB Code:

```
int fsrPin = 0;     // the FSR and 10K pulldown are connected to a0
int fsrReading;     // the analog reading from the FSR resistor divider
int fsrVoltage;     // the analog reading converted to voltage
unsigned long fsrResistance;  // The voltage converted to resistance
unsigned long fsrConductance;
long fsrForce;       // Finally, the resistance converted to force
 void setup(void) {
  Serial.begin(9600);   // We'll send debugging information via the Serial monitor
}
void loop(void) {
  fsrReading = analogRead(fsrPin);
  Serial.print("Analog reading = ");
```

```
Serial.println(fsrReading);
 // analog voltage reading ranges from about 0 to 1023 which maps to 0V to 5V (= 5000mV)
fsrVoltage = map(fsrReading, 0, 1023, 0, 5000);
Serial.print("Voltage reading in mV = ");
Serial.println(fsrVoltage);
if (fsrVoltage == 0) {
  Serial.println("No pressure");
} else {
  // The voltage = Vcc * R / (R + FSR) where R = 10K and Vcc = 5V
  // so FSR = ((Vcc - V) * R) / V        yay math!
  fsrResistance = 5000 - fsrVoltage;     // fsrVoltage is in millivolts so 5V = 5000mV
  fsrResistance *= 10000;                // 10K resistor
  fsrResistance /= fsrVoltage;
  Serial.print("FSR resistance in ohms = ");
  Serial.println(fsrResistance);
   fsrConductance = 1000000;           // we measure in micromhos so
  fsrConductance /= fsrResistance;
  Serial.print("Conductance in microMhos: ");
  Serial.println(fsrConductance);
   // Use the two FSR guide graphs to approximate the force
  if (fsrConductance <= 1000) {
    fsrForce = fsrConductance / 80;
    Serial.print("Force in Newtons: ");
```

```
      Serial.println(fsrForce);
    } else {
      fsrForce = fsrConductance - 1000;
      fsrForce /= 30;
      Serial.print("Force in Newtons: ");
      Serial.println(fsrForce);
    }
  }
  Serial.println("--------------------");
  delay(1000);
}
```

7) Effect of needle array on skin after TNT:

To test the effect of the needle array on dorsal murine skin, the TNT chip was placed on the skin after nairing and exfoliation. Supplementary Figure 6 shows the skin before (a) and after (b) TNT procedure. No signs of injury or inflammation was observed in the skin.

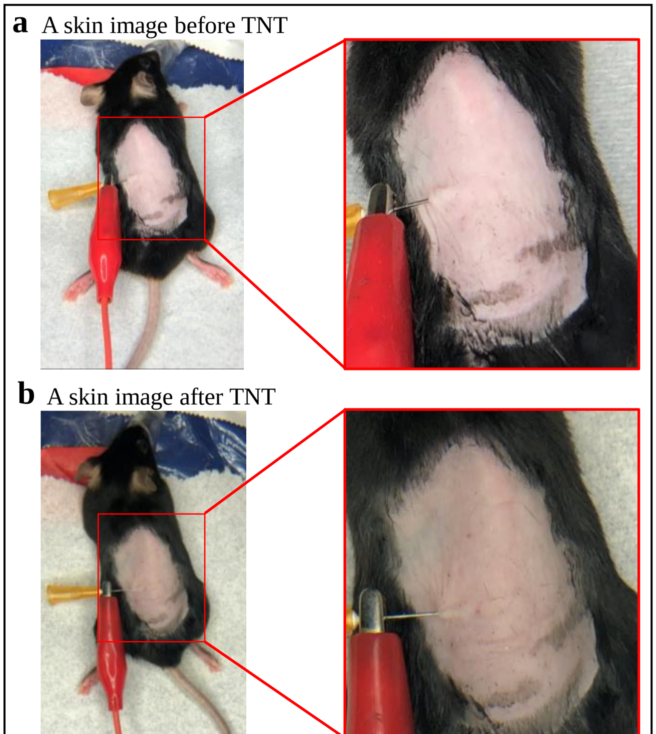

Supplementary Figure 6. Effect of needle array on skin after TNT (a) Pictures of the mouse before TNT procedure, (b) Pictures of the mouse after TNT procedure.

Supplementary Table 3: Individual data of gene expression in different animals post-TNT (related to Figure 11c)

		Fold Change		
ID	**Group**	**Ascl1**	**Brn2**	**Mytl1**
Animal 1	Control 1	0.1503	0.5151	0.6998
Animal 2	Control 2	3.1058	2.6900	2.8139
Animal 3	Control 3	0.6647	0.6041	0.4119
Animal 4	Control 4	0.0791	0.1908	0.0744
Animal 5	ABM-1	15.1137	11.6630	25.6228
Animal 6	ABM-2	73.3887	48.7377	54.7543
Animal 7	ABM-3	14.3818	8.8458	11.4739
Animal 8	ABM-4	38.5638	19.2369	24.5906

References

1. Wu, B.; Kumar, A.; Pamarthy, S., High aspect ratio silicon etch: A review. *Journal of Applied Physics* **2010,** *108* (5), 051101.

2. Na, Z.; Junjie, L.; Henry, R.; Lin, L.; Qifeng, J.; Junfeng, L., Deep silicon etching for thermopile structures using a modified Bosch process. *Journal of Micro/Nanolithography, MEMS, and MOEMS* **2019,** *18* (2), 1-6.

3. Tang, Y.; Sandoughsaz, A.; Najafi, K. In *Ultra high aspect-ratio and thick deep silicon etching (UDRIE)*, 2017 IEEE 30th International Conference on Micro Electro Mechanical Systems (MEMS), 22-26 Jan. 2017; 2017; pp 700-703.

4. Bates, R. L.; Goeckner, M. J.; Overzet, L. J., Correction of aspect ratio dependent etch disparities. *Journal of Vacuum Science & Technology A* **2014,** *32* (5), 051302.

5. Jo, S. B.; Lee, M. W.; Lee, S. G.; Lee, E. H.; Park, S. G.; O, B. H., Characterization of a modified Bosch-type process for silicon mold fabrication. *Journal of Vacuum Science & Technology A* **2005,** *23* (4), 905-910.

6. Juan, W. H.; Pang, S. W., High-aspect-ratio Si etching for microsensor fabrication. *Journal of Vacuum Science & Technology A* **1995,** *13* (3), 834-838.